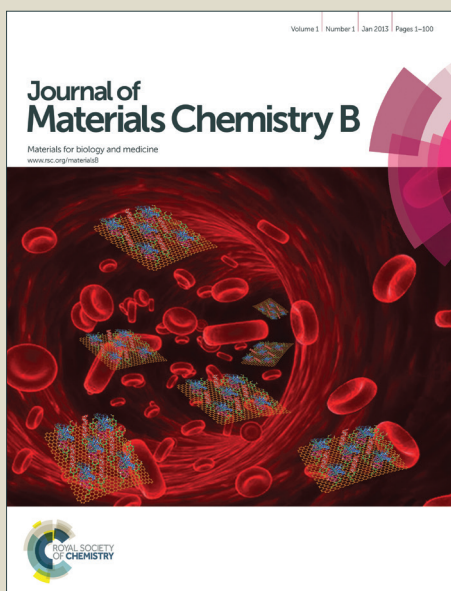


Journal of Materials Chemistry B

Accepted Manuscript



This is an *Accepted Manuscript*, which has been through the Royal Society of Chemistry peer review process and has been accepted for publication.

Accepted Manuscripts are published online shortly after acceptance, before technical editing, formatting and proof reading. Using this free service, authors can make their results available to the community, in citable form, before we publish the edited article. We will replace this *Accepted Manuscript* with the edited and formatted *Advance Article* as soon as it is available.

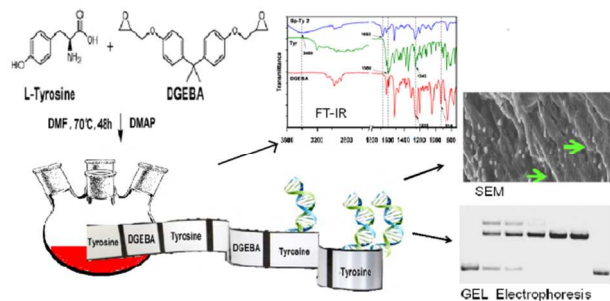
You can find more information about *Accepted Manuscripts* in the [Information for Authors](#).

Please note that technical editing may introduce minor changes to the text and/or graphics, which may alter content. The journal's standard [Terms & Conditions](#) and the [Ethical guidelines](#) still apply. In no event shall the Royal Society of Chemistry be held responsible for any errors or omissions in this *Accepted Manuscript* or any consequences arising from the use of any information it contains.

Table of Content Text

Monotyrosine based copolymer was synthesized, characterized and studied for its interaction with DNA for potential biological applications.

Table of Content Graphic



Cite this: DOI:

10.1039/c0xx00000x

www.rsc.org/xxxxxx

ARTICLE TYPE

Synthesis and characterization of biocompatible monotyrosine-based polymer and its interaction with DNA

Radhika Mehta,^a Rina Kumari,^a Prolay Das^a and Anil K. Bhowmick^{*a,b}

Received (in XXX, XXX) Xth XXXXXXXXX 20XX, Accepted Xth XXXXXXXXX 20XX

DOI: 10.1039/b000000x

ABSTRACT: A novel tyrosine-based copolymer containing L-tyrosine (Tyr) and diglycidylether of bisphenol A(DGEBA) was synthesized and studied for its interaction with DNA for potential applications in biological systems. The synthesis of the polymer was optimized by varying monomer ratios using 4-(dimethylamino)pyridine (DMAP) as catalyst to yield polymers with M_w of 7500-8000. Further characterization with FTIR, NMR and thermal analysis supported the formation of monotyrosine-DGEBA polymer. The interaction of 1:1 DGEBA-tyrosine copolymer with DNA was investigated by gel electrophoresis, thermal melting, and fluorescence spectroscopy in ratios ranging from 0.5:1 to 12:1 polymer–DNA (w/w). The copolymer was seen to lend stability to the DNA without damaging it and demonstrated endonuclease resistivity that is conducive for biological applications. Scanning Electron Microscopy, Dynamic Light Scattering and Zeta Potential studies of the polymer-DNA complex also established that the polymer is capable of encapsulating DNA leading to the formation of the DNA-polymer polyplex nano-assembly. The potential of the polymer for biological applications was further reinstated by its non-cytotoxicity.

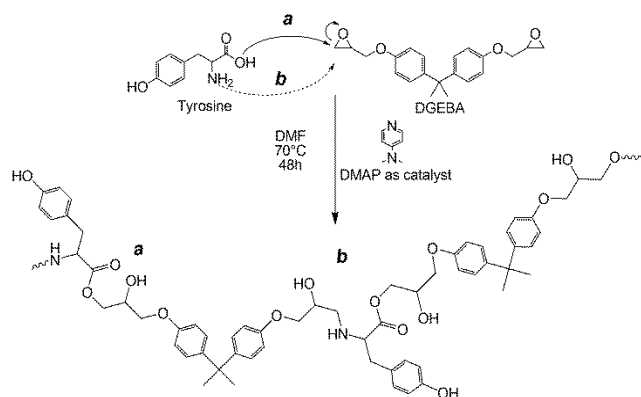
Introduction

Tyrosine, while classified as a non-essential amino acid, is used as a building block for several important neurotransmitters, including norepinephrine,¹⁻³ epinephrine³ and dopamine⁴ as well as play an important role in photosynthesis.⁵ Apart from its biological roles, researchers have used tyrosine as an amino acid of choice to create unique polymers and supramolecular structures.⁶⁻⁸ Such polymers have been researched for applications in various biomedical areas including tissue engineering, drug and gene delivery amongst others.⁹⁻¹² The choice of tyrosine for creating novel polymers stems from the unique structure of the neutral amino acid that harbours an aromatic ring and three functional groups that can be made to react with various reagents after careful manipulation of the reaction conditions.

Herein, we report the synthesis and characterization of a copolymer that incorporates tyrosine, with DGEBA as a linker through generation of ester and amine functionalities at linkages. The use of L-tyrosine as one of the main constituents of a copolymer with DGEBA has not been reported before to the best of our knowledge. Our synthetic methodology leads to the formation of a polymer that incorporates the less reactive, poorly soluble L-tyrosine with the highly hydrolysable DGEBA. The incorporation of DGEBA in the polymer is due to its ability to polymerize efficiently through its highly reactive epoxide moiety that can be easily broken in mild acidic or basic conditions. The π - π interaction between the aromatic rings of the constituents have been found to facilitate the formation of nanostructures

through the self-assembly of such polymers¹³ which also prompted us to investigate tyrosine in the context of polymerization with DGEBA. DGEBA has been extensively polymerized to generate copolymers with lactones and amines.^{14, 15} Synthesis of DGEBA homopolymer is also reported¹⁶ by anionic polymerization mechanism. Structure and properties of several copolymers have been discussed previously by one of the authors.^{17, 18}

Peripheral coupling of tyrosine to polycationic polymers has been achieved that displayed reduced cytotoxicity and stability for in-vitro and in-vivo applications.^{8, 13} Tyrosine polymerization resulting in the generation of dityrosine units in the polymer matrix have been reported with potential bio-application.^{9, 10, 19} As such, many tyrosine polymers have been found to be biocompatible by common cell cytotoxicity assays and many researchers have pointed out their potential bioapplications including drug delivery, gene delivery and tissue engineering.^{9, 11} However, low cytotoxicity essentially does not mean that the concerned polymer does not inflict any damage to biomolecules like DNA and scores of proteins inside the cell at the molecular level. The interactions of the polymers with important cellular contents need to be evaluated in detail to ensure safety of the cellular contents for the desired in-vitro or in-vivo applications. In this context, the interaction of tyrosine-based polymers with biomolecules like DNA and proteins at the molecular level is still largely unknown. Thus, apart from the synthesis and the meticulous characterization of the novel tyrosine-DGEBA polymer herein, we also report a detailed study



Scheme 1 Scheme showing the formation of the polymer by the reaction of DGEBA with tyrosine through (a) ester and (b) amine linkages via ring opening.

of the interaction of the synthesized tyrosine-DGEBA with various forms of DNA viz. calf thymus DNA (ctDNA), plasmid and DNA oligomer duplex of approximately 50 base pair long. Our study also discusses the non-cytotoxicity and the ability of the polymer to resist endonuclease activity on the DNA.

Experimental Section

Materials

Diglycidyl ether of bisphenol A (DGEBA), 4-(dimethylamino) pyridine (DMAP), L-Tyrosine (Tyr), calf thymus DNA (ctDNA), agarose, Ethidium bromide (EtBr) and chemicals for buffer preparation were purchased either from Sigma or Merck and used as received. The pUC19 plasmid and Hind III restriction enzyme were purchased from New England Biolabs, USA. All other materials and solvents were used as received without further purification. All experiments of polymer-DNA interactions were done in triplicate and error bars were generated after calculating the mean SD from the average value wherever applicable.

Synthesis of DGEBA-Tyrosine polymer

The optimized synthetic route is reported herewith (Scheme 1). Variations to solvent, catalyst, time, temperature and concentration of catalyst and monomers were also employed. Copolymers were synthesized by adding DGEBA to L-Tyrosine in varying monomer ratios of 1:0.5 (**Bp-Ty 1**), 1:1 (**Bp-Ty 2**) and 1:1.5 (**Bp-Ty 3**).

The synthetic route mechanistically involves ring opening of the DGEBA epoxide moiety with the activation of amine and carboxyl groups on tyrosine (Scheme 1). The synthesis for copolymer **Bp-Ty 2** employed for DNA interaction studies is as follows.

L-tyrosine (2 mmol, 0.3622 g) and DMAP (0.4 mmol, 0.0488 mg) were dissolved in 4-N,N-dimethyl formamide (DMF) (5 mL) in a 25 mL round bottom flask and heated to 70°C, to which, a solution of DGEBA (2 mmol, 0.6808 mg) in DMF (5 mL) was added drop wise with constant stirring. The reaction mixture was monitored with silica gel TLC in 60–40 ethyl acetate-hexane solvent system (by volume) that shows complete disappearance of DGEBA spot after 48 hours. The product was precipitated in water after solvent evaporation. A sticky brown solid separated out of the solution that was washed with water (5 X 10 mL) and

ether (5 X 5 mL) to remove DMF, DMAP and unreacted monomers. Crude product thus obtained was further purified by dissolving in DMF and precipitating with water in an ice bath (0°C), following water and ether washes and drying under vacuum for 24 hours. The method for re-precipitation was repeated twice to obtain ultrapure compound for polymer characterization and further downstream studies with DNA. Alternatively, the reaction mixture in DMF was concentrated under vacuum to a volume of 5 mL. To this, 20 mL cold methanol was added in an ice bath with stirring to precipitate out unreacted tyrosine. The extract was filtered and solvent evaporated to remove methanol and DMF. The polymeric product was then precipitated out in water as discussed above. ¹H-NMR (400 MHz, DMSO-d₆) δ: 1.5 (s, 6H), 2.2–3.0 (m, 5H), 3.1–4.5 (m, 12H), 6.2–8.0 (m, 12H). ¹³C-NMR (100 MHz, DMSO-d₆) δ: 30.72, 40.52, 41.11, 62.74, 67.29, 69.40, 69.95, 113.78, 115.03, 127.36, 129.94, 142.45, 142.82, 156.45, 162.30. ESI-MS m/z: 495.53 (Tyr+DGEBA-CO), 521.53 (Tyr+DGEBA-H), 227.40 (Bisphenol A fragment of DGEBA).

Variations to the above synthetic route were (a) use of tetrahydrofuran (THF) as solvent (b) use of triphenyl phosphine (TPP) and NaOH as catalysts at 10 mole percent (c) variation of DMAP concentration at 5 and 10 mole percent (d) variation of temperature from 25 to 100°C and (e) DGEBA-Tyr molar ratio at 1:0.5 (**Bp-Ty 1**) and 1:1.5 (**Bp-Ty 3**).

Characterization of polymers

Infrared spectroscopy was performed on Perkin-Elmer Spectrum-400 FTIR Spectrometer using KBr pellets in transmission mode in the spectral range 4000–650 cm⁻¹ with a total 16 scans per sample. ¹H-NMR (400 MHz) and ¹³C-NMR (100 MHz) were performed on Bruker Avance II FT-NMR Spectrometer using DMSO-d₆ as solvent and TMS as internal standard and chemical shifts are reported in δ-ppm scale. Molecular weight determination was carried out using Agilent PLGPC 50 Integrated Gel Permeation Chromatography (GPC) using PL gel 5 μm Mixed-D column equipped with a refractive index detector. The sample was prepared in HPLC-grade DMF and calibrated with polystyrene standards. Thermogravimetric analysis (TGA) was performed on TA SDT-Q600 under nitrogen atmosphere. Powdered samples were heated from 25 to 800°C at 10°C/min. The polymer and polymer-DNA complexes were imaged using a Field Emission Scanning Electron Microscope (FE-SEM) from Hitachi-S4800 (Tokyo, Japan). An accelerating voltage of 5 kV and working distance of 8 mm was used to image the samples. Electron spray Ionisation (ESI)- Mass Spectrometry was performed on Thermo LCQ Deca XP MAX in the negative modus with a m/z range of 100–1000.

Thermal Melting Studies

The stability of calf thymus DNA (ctDNA) in the presence of **Bp-Ty 2** was assessed by measuring the absorbance (A) at 260 nm (average time 1°C/min, ramp rate 0.5°C/min, from 90°C to 25°C and in reverse order) as a function of temperature (T) (dA/dT) on a Peltier controlled Bio Quest CE2501 spectrophotometer (Cecil, UK). Absorbance was measured with 50 μL aliquots containing 7.5 μg of ctDNA was mixed with the polymer in concentration ratios of 0.25:1, 0.5:1 and 1:1 in 10 mM sodium phosphate (NaPi) buffer at pH 7.4 in 5% DMSO.

Agarose Gel Assay

Polymer solution at the desired concentrations were mixed with 250 ng of pUC19 plasmid DNA and incubated at 37°C for 24 hours in 10 mM NaPi buffer (pH 7.4) with 5% DMSO (v/v).
5 These samples were then loaded into wells of 1% agarose gel (TAE buffer pH 8, 100 V, 1.5 h) and run with control samples as the plasmid DNA only. The DNA bands were visualised with ethidium bromide staining on UVP GelDoc-It 300 gel documentation system (UK). The quantitative estimation of the presence of supercoiled (SC), open circular (OC) or the linear (L), if any, was done using Vision Work Ls Image Acquisition and Analysis software from UVP (UK). A nuclease resistance assay was also carried out to evaluate the stability of the DNA in the polymer-DNA complex against restriction enzyme Hind III.
15 The polymer/DNA complex and free DNA were separately incubated with Hind III buffer including Hind III (2 Units/250 ng DNA) at 37°C for 1 h. The results were analyzed by 1% agarose gel electrophoresis.

EtBr Displacement Assay

Fluorescence studies involving EtBr displacement from DNA in presence of the polymer were recorded on a Horiba Jobin Yuon Floromax-4 spectrofluorometer at excitation and emission wavelengths of 540 nm and 600 nm respectively. Each aliquot
25 (50 µL) containing 30µM pUC19 DNA and 5µM EtBr incubated for 12 hours with **Bp-Ty 2** in different ratios in 10 mM NaPi buffer at pH 7.4 with 5% DMSO (v/v). Fluorescence of pure EtBr and DNA-EtBr were also recorded under the same conditions. The percentage of relative fluorescence upon polymer binding
30 was calculated using the following equation:²⁰

$$\text{Percentage of relative fluorescence} = \frac{(F_{\text{obs}} - F_0) \times 100}{(F_{\text{DNA}} - F_0)} \quad (1)$$

where F_0 , F_{DNA} and F_{obs} are the fluorescence intensities of unbound EtBr, EtBr intercalated with plasmid DNA and EtBr-DNA complex with polymer respectively.
35

Particle Size and Zeta Potential Determination

The hydrodynamic diameter and zeta potential of the polymer-DNA complexes were measured by Dynamic Light Scattering (DLS) experiments on a Delsa NanoC Particle Analyser
40 (Beckman-Coulter). Individual samples of ctDNA (15 µg/mL) in 1 mM NaPi at pH 7.0 (2 mL) filtered through a membrane filter (PVDF, 0.2 µm) were prepared and aliquots of polymer solutions in DMSO were added to achieve different polymer-DNA (w/w) ratios with an overall 5% DMSO (v/v) in 1 mM NaPi buffer at
45 pH 7.0. The DLS measurements were performed after 30 minutes and as well as after 12 hours incubation in duplicate at 25°C and a scattering angle of 165°. The average particle size of each sample was obtained by using CONTIN analysis as the mean hydrodynamic diameter (standard deviation of five
50 determinations including polydispersity). For zeta potential measurements, polymer-DNA complexes at ratios of 1:1, 1:5, 1:10 and 1:20 containing 2.5µg/mL ctDNA were prepared in distilled water with 5% DMSO (v/v). These were incubated for 12 hours and the zeta potential was measured across electric field

55 of 16.3 V/cm, scattering angle of 15° and cell positions of 0 mm, ±0.35 mm and ±0.7 mm.

MTT Assay for Cell Activity

The MTT assay was performed to measure the metabolic activity of cells. 1 mg of **Bp-Ty-2** was dissolved in 0.5 mL of 5% DMSO
60 to make 2 mg/mL stock solution. The stock solution was diluted to 100 µg/mL, 75 µg/mL, 50 µg/mL, 25 µg/mL and 10 µg/mL concentration solutions in the culture medium with serum. Cells cultured in normal medium were considered as cell control and 5% DMSO in culture medium as reagent control (0.5% DMSO).
65 Equal volume (100 µL) of various dilutions of test samples, extract of negative control UHMWPE (ultra high molecular weight polyethylene), cell control, reagent control and positive control (dilute phenol) were placed on subconfluent monolayer of L-929 cells (mouse fibroblast). After incubation of the cells with
70 various concentration of the test samples and controls at 37°C±1°C for 24 hours, extract and control medium was replaced with 50 µL MTT solution (1 mg/mL in medium without supplementary), wrapped with aluminium foil and were incubated at 37°C±1°C for 2 hours. After discarding the MTT solution, 100
75 µL of isopropanol was added to all the wells and subsequently the color developed was quantified by absorbance measurement at 570 nm. The data obtained for test sample, reagent control negative control (UHMWPE) and positive control (dilute phenol) were compared with cell control.

80 Results and Discussion

Synthesis of Tyrosine-DGEBA polymers

Polymerization of tyrosine and DGEBA is hypothesized to proceed via nucleophilic attack of DMAP on tyrosine to facilitate its activation and the ring opening of the DGEBA epoxide moiety
85 (Scheme 1). Tyrosine, having low solubility in most organic solvents, is appreciably soluble in aqueous solvents depending on pH. It exists primarily in zwitterionic form, and hence is not readily reactive. The reaction between tyrosine and DGEBA was carried out in an organic medium as the epoxide moiety of
90 DGEBA gets hydrolyzed in aqueous solution. Initial reactions were performed using tetrahydrofuran as solvent. However, low solubility of tyrosine in THF led us to employ DMF as the solvent.

The reaction in DMF with 1:1 monomer ratio (**Bp-Ty 2**) was monitored until the consumption of at least one of the monomers. The reaction was followed for 48 hours at 70°C when disappearance of DGEBA spot on TLC and no sedimentation of unreacted tyrosine were observed. The reaction at 16 hours and 24 hours at 10% DMAP concentration showed DGEBA spot on
100 TLC and sedimentation of excess tyrosine indicative of incomplete reaction. It is apparent from Figure 1A that the tyrosine consumed in the reaction is linearly proportional with time up to 50 hours. The higher the catalyst concentration, the higher is the slope or higher is the reaction rate (Figure 1A, 1B).
105 5 mole percent DMAP concentration gave only 15% yield compared to 58% with 10 mole percent DMAP at 48 hours and 70°C. DMAP was not used at concentrations above 10% to avoid its embedding

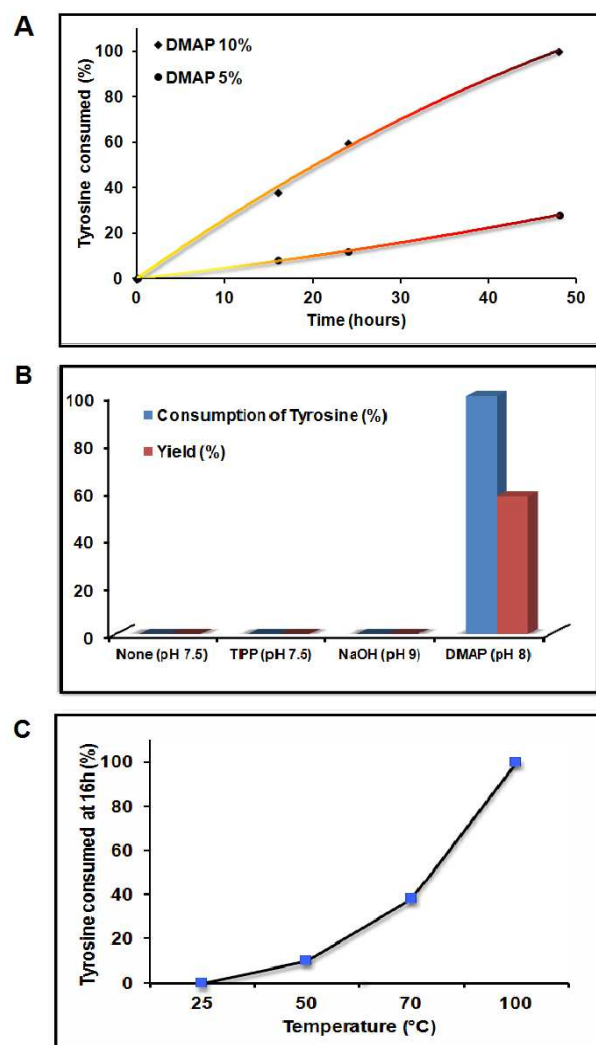


Fig. 1 (A) Plot showing percentage consumption of tyrosine from the reaction mixture with time for 1:1 molar ratio of monomers at varying DMAP concentrations. The colour gradient of the curve resembles the reaction mixture at the respective time intervals (B) Progress of the reaction between DGEBA and Tyrosine with choice of catalyst and pH as a function of Tyrosine consumption and yield (C) Plot showing consumption of tyrosine as a function of temperature.

in the polymer matrix. With 5% catalyst, excess tyrosine sediments out of the reaction and TLC confirmed presence of excess DGEBA in the solution, indicating that 10 mole percent DMAP was required for complete consumption of the reagents (Figure 1A).

The reaction between tyrosine and DGEBA was initially performed without any catalyst, with variations to temperature from 25, 40 to 70°C without any yield. Excess tyrosine was seen to sediment in the flask at the end of each reaction. Thus, an initiator/catalyst was employed such that it may catalyze the reaction. NaOH and triphenyl phosphine (TPP) were also used, at 10 mole percent in the basic pH range. Both failed to digest tyrosine in the reaction (Figure 1B) unlike DMAP, which demonstrated consumption of tyrosine and change in colour of solution from a white colloidal mixture to dark brown clear solution indicating reaction between tyrosine and DGEBA.

Temperature variation was carried out to ascertain the

dependence of the reaction on temperature. As seen from Figure 1C, the reaction proceeds faster on increasing the temperature. At room temperature, the reaction failed to proceed, indicating the need to heat to activate the reaction. On going from 70 to 100°C, complete consumption of tyrosine was observed at the end of 16 hours.

Reaction with lower ratios of tyrosine-DGEBA (**Bp-Ty 1**) showed presence of residual DGEBA as confirmed by TLC. However, no sedimentation of tyrosine was observed indicating complete addition of tyrosine to the polymer matrix. For **Bp-Ty 3**, i.e. at a higher ratio of tyrosine: DGEBA, sedimentation of excess tyrosine at the end of 48 hours was observed. Thus, this reaction occurs primarily in 1:1 molar ratios of DGEBA-Tyr which has been the focus of our study with DNA.

The polymerization method employed also generates DGEBA homopolymer but failed to homopolymerize tyrosine. The DGEBA homopolymer was light yellow in colour and insoluble in common organic solvents including MeOH, DCM, THF, Hexane, CHCl₃, DMF and DMSO. In contrast, the synthesized copolymers **Bp-Ty 1, 2 and 3** were brown in colour and soluble in organic solvents including DMF, DMSO and a mixture of MeOH-DCM, which supports the fact that the synthesized polymer is a copolymer comprising of both DGEBA and tyrosine. Further characterization of the synthesized copolymers via GPC, FTIR, NMR and TGA are discussed below.

Molecular Weight Determination

Gel Permeation Chromatography

The molecular weights of the synthesized polymers were determined using GPC as tabulated below (Table 1). The 1:1 DGEBA-Tyr (**Bp-Ty 2**) copolymer had Mw of 7800 and a polydispersity index (PDI) of 1.21. The GPC data for polymers – **Bp-Ty 1** and **Bp-Ty 3** indicate similar molecular weight range for higher and lower tyrosine ratios. With a low PDI of 1.2, there is an indication that the synthesized polymers are not branched. **Bp-Ty 2** is hypothesized to consist of 12-15 units each of tyrosine and DGEBA as an AB type random copolymer, which is further supported, by NMR, ESI-MS and thermal studies.

Table 1 Molecular weight and polydispersity determination using GPC

Sample	Mn	Mw	PDI
Bp-Ty 1, 48h, 70°C	6450	7800	1.21
Bp-Ty 2, 48h, 70°C	6230	7560	1.21
Bp-Ty 3, 48h, 70°C	6410	7780	1.21

Mass Spectrometry

The ESI-MS spectra for **Bp-Ty 2** (Supporting Information, Figure S1) copolymer shows major fragments at 495 Da (m/z) corresponding to 1 unit each of DGEBA and tyrosine with the loss of a CO moiety, 521 Da (m/z) for a complete DGEBA-Tyr unit and 227 Da (m/z) for bisphenol A moiety of DGEBA. The data show that the linkage between tyrosine and DGEBA results due to the ring opening of the epoxide moiety and its reaction with the carboxyl and amine groups of tyrosine without the loss of any water molecule. This supports the absence of any peptide linkage (between two tyrosine units) in the copolymer. This data also confirms that the major repeating unit in the polymer is Tyrosine-DGEBA.

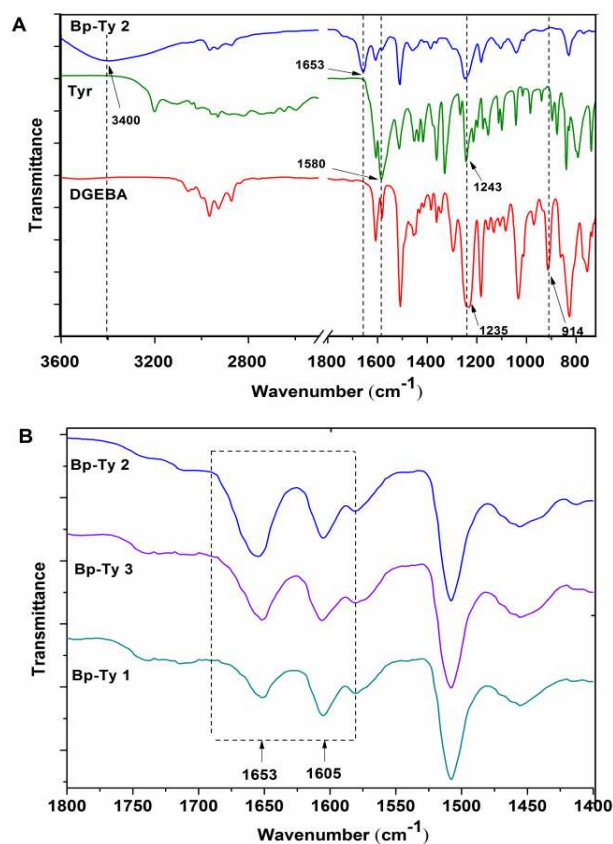


Fig. 2 (A) FTIR Spectra for pristine DGEBA, Tyrosine and **Bp-Ty 2** copolymer (B) FTIR Spectra for **Bp-Ty 1**, **2** and **3** with reference to the peak at 1653 cm^{-1}

5 Spectroscopic analysis of Tyr-DGEBA copolymers

Fourier Transform Infrared Spectroscopy

The IR spectrum for **Bp-Ty 2** copolymer (Figure 2A) shows

absorption peaks at 3400 cm^{-1} (medium, broad, hydroxyl groups and secondary amines), 1653 cm^{-1} (strong, carbonyl group- ester or amide group with tyrosine), 1605 cm^{-1} (strong, aromatic C=C), 1580 cm^{-1} (medium, aromatic C=C and N-H bend from tyrosine), 1505 cm^{-1} (strong, aromatic C=C), 1243 cm^{-1} (strong, broad, C-N stretch for tyrosine) and 1235 cm^{-1} (C-O-C bend for DGEBA). Disappearance of the characteristic peak of DGEBA at 914 cm^{-1} for epoxide bending indicates ring opening of the DGEBA moiety. The strong peak appearing at 1653 cm^{-1} in the product is an indication of the formation of a carbonyl group in the copolymer.

The peak at 1653 cm^{-1} was normalized with respect to the 1605 cm^{-1} peak (C=C stretching in aromatic compounds) for the synthesized **Bp-Ty** copolymers. As depicted in Figure 2B, this peak had high transmittance for **Bp-Ty 2** and **Bp-Ty 3**. As expected, the transmittance decreased for 1:0.5 DGEBA-Tyr (**Bp-Ty 1**) copolymer due to low amount of tyrosine incorporated in the polymer.

Nuclear Magnetic Resonance Spectroscopy

The peaks corresponding to the functionalities are shown in the NMR spectra (Figure 3).

In the $^1\text{H-NMR}$, the protons are accounted for in the 4-9 ppm range. For amide functionality, a peak between 4-6 ppm is expected²¹ that is absent here, indicative of ester bonding between tyrosine and DGEBA, which correlates with the mass spectrometry result discussed previously. The monomeric ratios in the synthesized copolymers were calculated from the NMR spectra by taking a ratio of the number of aliphatic methyl protons of DGEBA to aromatic protons of DGEBA and Tyrosine. With a substrate ratio of DGEBA-Tyr as 1:1, the ratio of aliphatic methyl protons to aromatic protons was calculated as 6:12 or 1:2. The NMR spectrum for the synthesized polymer **Bp-Ty 2** (Figure 3B), displays this aliphatic to aromatic proton ratio close to 1:2.

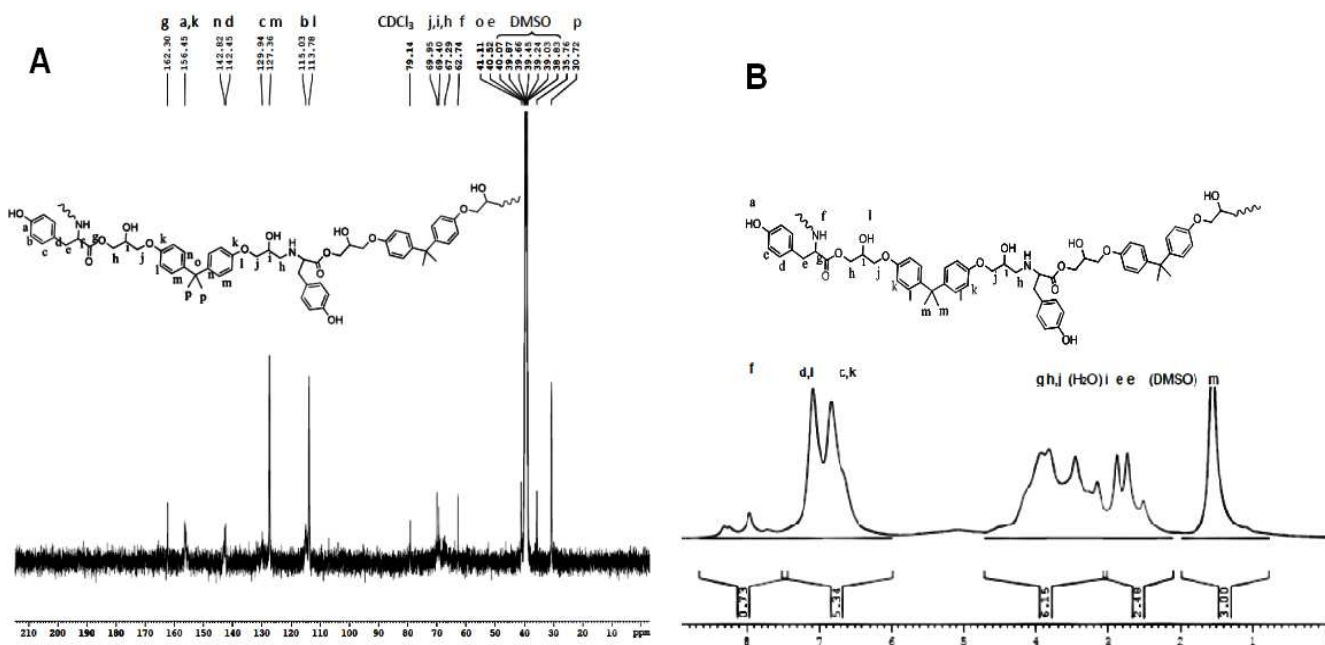


Fig. 3 NMR spectra of the synthesized polymer **Bp-Ty 2** (A) ^{13}C NMR spectra (B) ^1H NMR spectra

Cite this: DOI:

10.1039/c0xx00000x

www.rsc.org/xxxxxx

ARTICLE TYPE

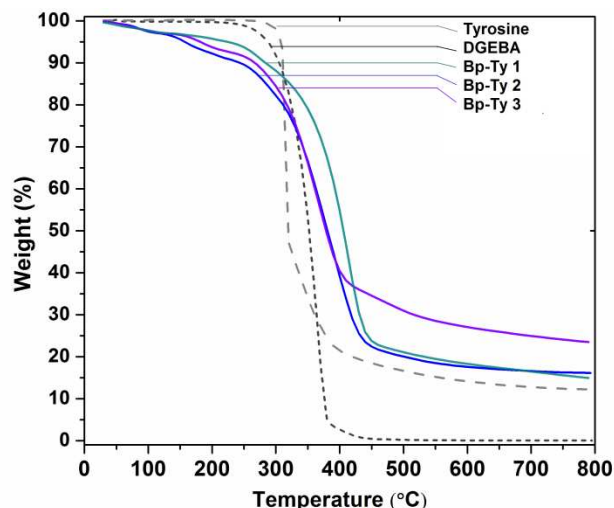


Fig. 4 TGA curve showing thermal degradation of **Bp-Ty 1, 2 and 3** with respect to the monomers DGEBA and tyrosine.

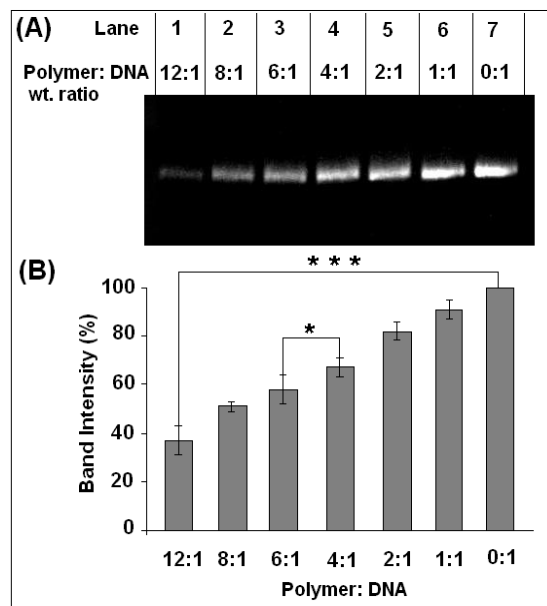


Fig. 5 Effect of polymer on the supercoiled form of pUC19 plasmid DNA after incubation for 24 hours. (A) 1% Agarose gel showing results of incubation of plasmid with **Bp-Ty 2** in various weight ratio. No relaxed or linear form was detected. (B) Quantitative estimation of decrease of intensity of plasmid band in the agarose gel due to groove binding of the polymer with DNA. Each value represents mean \pm SD. An * denotes a statistical significance of $p < 0.005$ and *** denotes a statistical significance of $p < .00001$ between samples as measured by unpaired t-test.

Thermal Analysis of Tyrosine-DGEBA Copolymers

Thermogravimetric Analysis (TGA) was performed on the synthesized copolymers to study the effect of temperature on degradation. TGA curves for the **Bp-Ty 1, 2 and 3** are shown in

Figure 4. The derivative curves for the copolymers (Supporting Information, Figure S2) were analyzed²² to determine ratios of tyrosine (320°C, 50% degradation) and DGEBA (370°C, 95% degradation) in the sample with reference to the monomers. The calculated Tyr:DGEBA ratios for **Bp-Ty 1**, **Bp-Ty 2** and **Bp-Ty 3** are 0.49:1, 1:1 and 1.1:1 respectively. This data indicates that even with a higher ratio of tyrosine as substrate, the amount of tyrosine remains equimolar to DGEBA. This was evident from the sedimentation of excess tyrosine at the end of the synthesis route for **Bp-Ty 3**. At 0.5:1 Tyrosine-DGEBA ratio (**Bp-Ty 1**), the synthesized copolymer contains monomers in the same ratio, which is supported by the fact that DGEBA undergoes homopolymerization in the above method. This also indicates the presence of copolymer units and DGEBA homopolymer within the polymer matrix of **Bp-Ty 1**. The copolymer **Bp-Ty 2** has a T_g centred at 77°C after which the copolymer starts to melt beyond 120°C (Supporting Information, Figure S3).

DGEBA-Tyrosine polymers do not damage DNA

Agarose gel assay was conducted to determine the effect of copolymer on DNA structure.

The supercoiled form of pUC19 plasmid DNA after incubation with the polymer does not show the presence of any linear or nicked form even after incubation for 24 hours (Figure 5A). This result corroborates the findings of Tseng et al. where poly(esterurethane) and poly(amino ester glycol urethane) polymers showed a similar effect.²³ However, in the present study with increase in polymer concentration, the intensity of the supercoiled plasmid band gradually decreased in the gel (Figure 5B). For polymer to DNA ratio of 1:1, decrease in the intensity of the band was ca. 10% which further decreased by ca. 63% when compared to the plasmid only control band in the agarose gel with increase in polymer concentration.

Further, we compared the band intensity and mobility pattern of DNA in agarose gel preincubated with the **Bp-Ty** polymer (neutral polymer) and poly(ethyleneimine) (PEI) (Mn 10000), a highly research polycationic polymer for delivery applications. The results are similar where the disappearance of DNA bands in agarose gels were observed, albeit at lower concentrations and incubation time in the case of PEI (Figure S4, Supplementary Information). Additionally, mobility shift of the DNA bands incubated with **Bp-Ty** was not observed whereas DNA incubated with PEI shows mobility shift at concentration ratio of 0.75:1 polymer-DNA (w/w). This suggests that PEI tends to neutralise the peripheral charge of DNA at lower concentrations due to its polycationic nature. Since the agarose gels were stained with EtBr after completion of the gel run, the decrease in the intensity of the plasmid bands is attributed to insufficient intercalation of the EtBr into DNA due to the shielding effect of the polymer on DNA at higher concentrations. The band for the supercoiled plasmid does not show any mobility shift, indicative of absence of any unwinding in the DNA brought about by the polymer. Thus, conformational destabilization in DNA is not being

introduced by the **Bp-Ty** polymer.

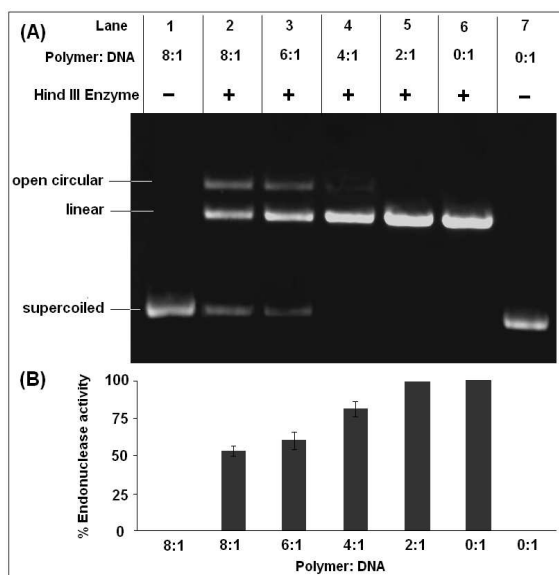


Fig. 6 Cleavage efficiency of restriction endonuclease Hind III on pUC19 plasmid DNA (A) 1% Agarose gel (pH 7.5) showing effect of different concentrations (w/w) of **Bp-Ty 2** on the endonuclease activity of Hind III following 24-hour incubation with pUC19. (B) Quantitative estimation of **Bp-Ty 2** induced resistance to endonuclease activity of Hind III on pUC19.

Table 2 Melting temperature (T_m) as determined from the thermal melting curve.

DNA-polymer ratio (w/w)	1:0	1:0.25	1:0.5	1:1
T_m ($^{\circ}\text{C}$)	66.0	66.9	68.5	71.0

The absence of any nuclease activity and unwinding of the DNA in presence of the polymer is a good indication that the polymer does not inflict any damage or modification to the DNA, which is desired for any biological application. The effect of the restriction enzyme, Hind III on the polymer-DNA complex to determine endonuclease activity is shown in Figure 6. Plasmid DNA, after incubation with the polymer at higher concentrations resists endonuclease activity of the enzyme Hind III to an appreciable degree (Figure 6A). As seen from Figure 6A, the free DNA (Lane 7) is completely linearized in the presence of Hind III. While up to polymer to DNA ratio of 2:1, the nuclease activity of Hind III remained unhindered, thereafter a gradual decrease in the nuclease activity of Hind III with increase in polymer concentration was observed. The nuclease activity of Hind III was reduced to ca. 50% at polymer concentration 8 times more

than the plasmid concentration (Figure 6B).

The decrease in nuclease activity suggests that at higher polymer concentrations, the DNA strands are not exposed to the surrounding due to shielding and encapsulation effect of the polymer that prevents recognition of DNA bases by the endonucleases giving rise to insufficient amount of the linear form of the plasmid.²³ To check whether the polymer has any effect on Hind III enzyme, the enzyme was co-incubated with the polymer at higher concentration followed by dialysis of the solution and incubation of the purified enzyme with DNA. No effect on the endonuclease activity of Hind III was observed, which further confirms the fact that interaction of the polymer with DNA is responsible for inhibition of endonuclease activity. This result is noteworthy since in the light of the possible use of any DNA cargo to be transported to a particular cellular location, the presence of numerous endogenous nucleases can degrade the DNA even before being released from the polyplex, thus rendering the delivery ineffective. In this case, the polymer can offer some resistance to endonuclease activity to the DNA cargo, albeit at higher concentrations.

DGEBa-Tyrosine copolymer lends stability to the DNA

Increase in DNA melting temperature (T_m) followed by addition of a compound or polymer is indicative of increase in the thermal stability of the DNA because of intercalation, groove binding, etc. The melting temperatures of the complexes formed between ctDNA and polymer at different ratios is shown in Table 2. The T_m of native ctDNA was observed at 66°C , and a gradual increase in the T_m was documented, up to 71°C with 1:1 weight ratio of polymer to DNA. A reference thermal melting data obtained to determine the effect of DMSO on T_m (not shown) showed a decrease in T_m to 65.5°C . However, the highest increase in melting temperature on complexation was found with the DNA-polymer ratio of 1:1 that confirmed the stabilisation of the DNA in the presence of the the copolymer (Table 2). However, sharp T_m was unavailable at higher polymer concentrations, possibly due to formation of higher order structures and aggregates.

Partial Intercalation of polymers into DNA replaces EtBr

The EtBr replacement assay was performed to measure the degree of association of the polymer with DNA (Figure 7). The decrease in fluorescence of EtBr intercalated into DNA results from the quenching of EtBr after it comes out from the DNA into the solvent.²⁴ A gradual decrease in the fluorescence of EtBr was observed upon the addition of the polymer.

Cite this: DOI:

10.1039/c0xx00000x

www.rsc.org/xxxxxx

ARTICLE TYPE

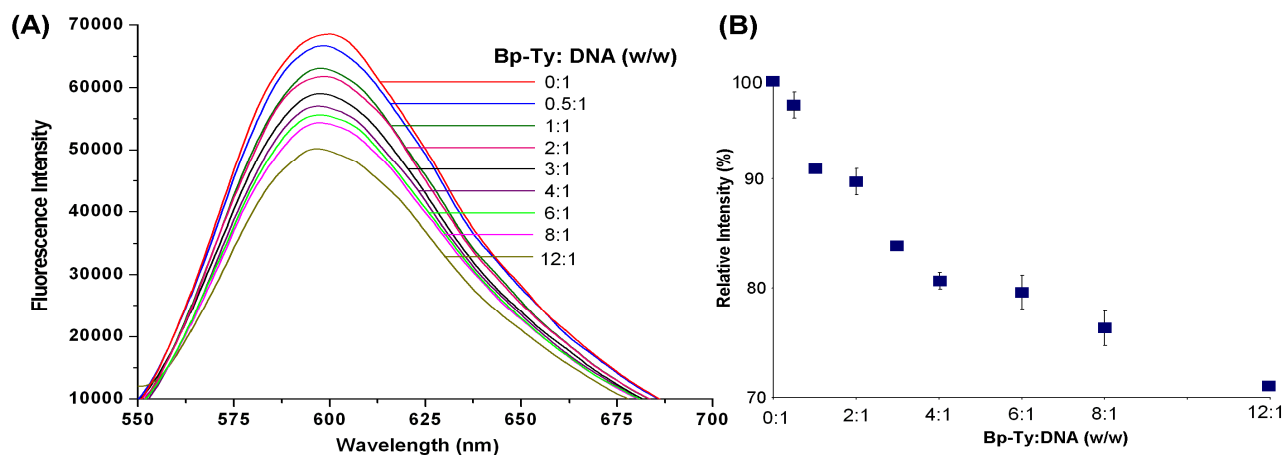


Fig. 7 EtBr displacement assay. (A) Decrease in Fluorescence intensity upon addition of **By-Ty 2** to DNA observed at $\lambda_{\text{ex}} = 540$ nm and $\lambda_{\text{em}} = 600$ nm. (B) Plot of relative fluorescence intensity with of DNA-EtBr at different polymer concentrations.

As observed from Figure 7, EtBr fluorescence is seen to decrease by nearly 30% only when the DNA and the polymer ratio is 12:1. This decrease in fluorescence is attributed to partial intercalation, thereby releasing bound EtBr in solution. The presence of other non-covalent interactions between polymer and DNA may also introduce change in DNA conformations, thereby releasing bound EtBr. Insertion of aromatic residues of the polymer between base pairs of DNA may lead to bending of the helix at the point of intercalation, essentially releasing EtBr and hence the decrease in fluorescence.²⁵ Most notably, the replacement of intercalated EtBr is not substantial at comparable DNA and polymer ratio. This observation points to the fact that at lower concentrations of the polymer, its intercalation into DNA is negligible, which means that the conformational distortion leading to DNA damage is minimal under such condition.

The data correlate well with the agarose gel assay data (Figure 5) wherein a gradual decrease in band intensity is observed on

increasing amount of the polymer. Thus, the DNA-copolymer complex formed is shown to be stable, with efficient binding and ability to restrict endonuclease degradation as desirable for a biocompatible material.

25 **Size and surface charge determination of polymers in presence of DNA**

The size and the surface charge of the polymer in presence of the DNA were investigated with DLS. As depicted in Figure 8A, good correlation was not obtained with only DNA or the polymer. However, upon addition of the polymer to DNA, the correlation function gets stabilized that indicate formation of stable particles of finite size. The same trend was observed with the intensity distribution, where only the DNA or the polymer had broad distributions that consequently narrowed down when co-incubated at respective concentrations (Figure 8B).

Cite this: DOI:

10.1039/c0xx00000x

www.rsc.org/xxxxxx

ARTICLE TYPE

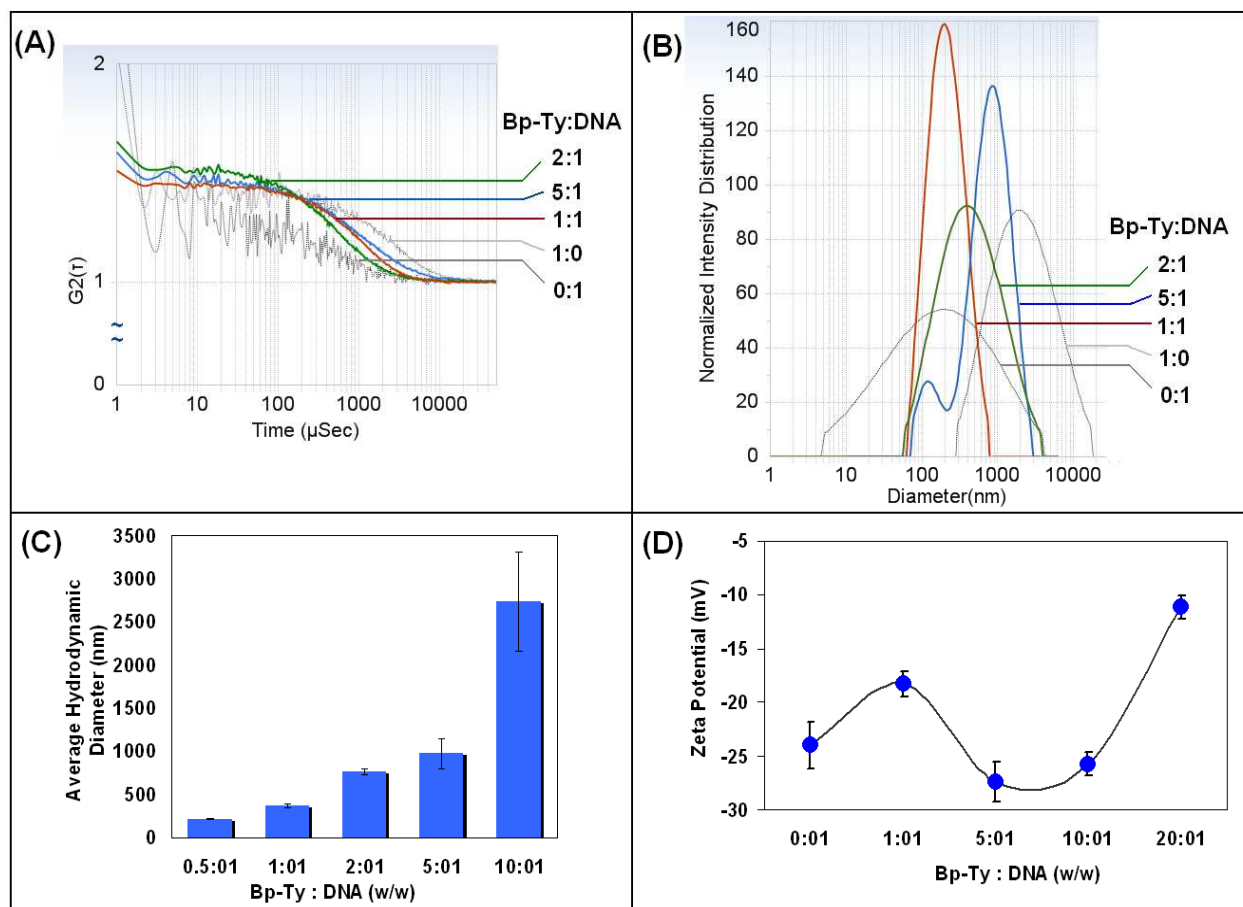


Fig. 8 Dynamic Light Scattering Experiments (A) Correlation factor for measurement of hydrodynamic diameter by incubating different concentrations of **Bp-Ty 2** to a definite concentration of DNA (B) Plot of Intensity distribution of DNA-polymer complexes with their respective hydrodynamic diameter. (C) Plot of average hydrodynamic diameter with different Polymer to DNA ratio after 12 hour incubation. (D) Measurement of Zeta potential at different Polymer to DNA ratio after 12 hour incubation

Hydrodynamic diameter of DGEBA-Tyr copolymer-DNA complexes at various copolymer to DNA w/w ratios was measured using DLS after incubation for 30 min (Supporting Information, Table S1) as well as after 12 hours (Figure 8C). Our results indicate possible formation of polyplex between the polymer and the DNA. A gradual increase in the hydrodynamic diameter of the polyplex was observed until polymer concentration was 5-6 times that of DNA. Our study shows that even after incubation of the DNA with the polymer for 12 hours, the polyplexes are stable as evident from the correlation and the particle size distribution. This is in contrast with PEI incubated DNA where aggregation is more prominent after 12 hours of incubation that can deter data acquisitions. In the present case of **Bp-Ty** polymer, there is a gradual increase in the average hydrodynamic radii whereas with PEI the hydrodynamic radii increases with increase or decrease in polymer concentration after 2:1 PEI-DNA ratio (w/w)²⁶. It is to be noted that DLS data with PEI and DNA could only be obtained after addition of relevant

concentration of NaCl unlike **Bp-Ty** polymer. Nevertheless, the average hydrodynamic radii of DNA condensates obtained by incubating with Bp-Ty polymer and PEI (Mn 10000) were found to be similar (~300 nm in the concentration range 5:1 w/w).

The best results in terms of correlation and intensity distribution was obtained when the concentration of polymer is between 1 to 5 times greater than the DNA. The sudden increase of the diameter at polymer concentration 10 times more than the DNA suggests formation of aggregates at such concentrations. This is hypothesised to be due to the condensation of polymeric sheets with DNA leading to a more linearized complex. At 0.5:1 polymer to DNA ratio, the hydrodynamic diameter is around 219 nm with standard deviation and polydispersity of 3 nm and 0.2 respectively indicating a uniform entity. With increasing polymer ratio to 1:1, the polydispersity and scattering intensity remain the same, but the diameter increases, which is in agreement with literature.²⁰ At higher ratios of polymer to DNA such as 10:1, the polydispersity is seen to increase significantly indicating a higher

degree of aggregation. Overall, stable particle formation was observed within a certain range of polymer concentration with DNA that shows appreciable interaction between the polymer and DNA. Comparison of the DLS data obtained after incubation of the DNA with the polymer for 30 minutes and 12 hours revealed some interesting differences (Supporting Information, Table S1). On incubation for 30 minutes, the hydrodynamic radii of the particles formed with a certain ratio of polymer to DNA, are smaller as compared to those incubated for 12 hours, indicating slow aggregation with time. It is also to be noted that the diameter observed in DLS is the average hydrodynamic diameter and not the actual diameter of the polyplex, which is proven to be much lesser than that of the hydrated form.²⁷ Zeta potential was recorded for copolymer-DNA complexes to gain insight about the complexes' surface charge and its potential stability. Effective charge density is considered as a crucial parameter in determining the structure and morphology of DNA in the condensed state. DNA condensation occurs when ~90% of the surface negative charge of DNA is neutralized in an aqueous solution and that is irrespective of the side chain functionality of the condensing agent.²⁸ The observed pKa of the polymer at 7.6 and 11.3 (Supporting Information, Table S2) confirms 80-100% ionization of the polymer according to Henderson-Hasselbalch equation, thereby supporting DNA condensation leading to the formation of the polyplex. The zeta potential results show that the free polymer has a zeta potential of 17 mV, possibly due to the basicity of the amine groups of tyrosine. The positive zeta potential for the polymer is also indicative of few free hydroxyl and carboxyl moieties in the polymer matrix. The surface charge for free DNA was observed to be -23.7 mV which is expected due to the phosphate groups on DNA. Zeta potential for the polymer-DNA complexes became negative after incubation indicating that the phosphate groups on DNA interact with the free amine groups thereby making the whole entity negative. It has also been reported earlier that the condensed DNA may well exist as partially dissociated polyanion, effectively bringing down the zeta potential.²⁹

As evident from Figure 8D, the zeta potential stabilized for 5:1 and 10:1 polymer to DNA ratios at a negative value, indicating the presence of free phosphate groups for binding. With further increase in polymer concentration, a decrease in zeta potential

was observed due to the availability of fewer free phosphate groups coupled with the fact of higher degree of aggregation and low stabilisation of the polyplex. The 20:1 complex was observed to be least stable as expected.

Imaging studies with DNA via SEM

The morphology of the copolymer-DNA complexes formed at ratio of 0.5:1 was examined using FE-SEM. The images of pure polymer were also obtained for reference (Figure 9A and 9B).

The **Bp-Ty 2** polymer had a sheet-like appearance with protrusions (50-100 nm) to the single-layered epoxy sheets. After incubation with DNA, the polymer sheets start aggregating around the DNA. In the SEM image for 0.5:1 polymer-DNA complex (Figure 9C and 9D), dense globular DNA fragments are observed. The morphology of the polymer sheet also changes after DNA interaction, showing smooth and rough patches. The smooth patches are attributed to free polymer. The rough patches as seen in Figure 9D are clusters of DNA spread throughout the polymer. The SEM images for 0.5:1 polymer-DNA polyplex display DNA on the surface of the polymer as well. For 1:1 polyplex (Figure 9E and 9F), the DNA could hardly be seen on the surface of the polymer sheet possibly due to its encapsulation by the polymer. As seen in Figure 9F, the DNA is much more discreetly spread out than in 9D. Thus, the SEM images of copolymer-DNA show DNA clusters and free polymer indicating that there are portions on the polymer that are not engaged in DNA interaction, which increase with polymer concentration. This also supports the agarose gel and EtBr experiments portraying the entrapment of DNA within the polyplex with increasing polymer concentration.

The interaction of DNA with the polymer at the interface and as a whole entity is pictorially depicted in Scheme 2. In summary, the polymer does not show any noteworthy nuclease activity and even protects plasmid DNA from endonuclease activity. Partial displacement of EtBr from DNA and elevated T_m were observed following incubation of the polymer with ctDNA. As deduced from SEM, the DNA is assembled in clusters and entrapped within the polymer matrix. DLS studies showed concentration dependant stable particle formation with ctDNA in the presence of the copolymer.

Cite this: DOI:

10.1039/c0xx00000x

www.rsc.org/xxxxxx

ARTICLE TYPE

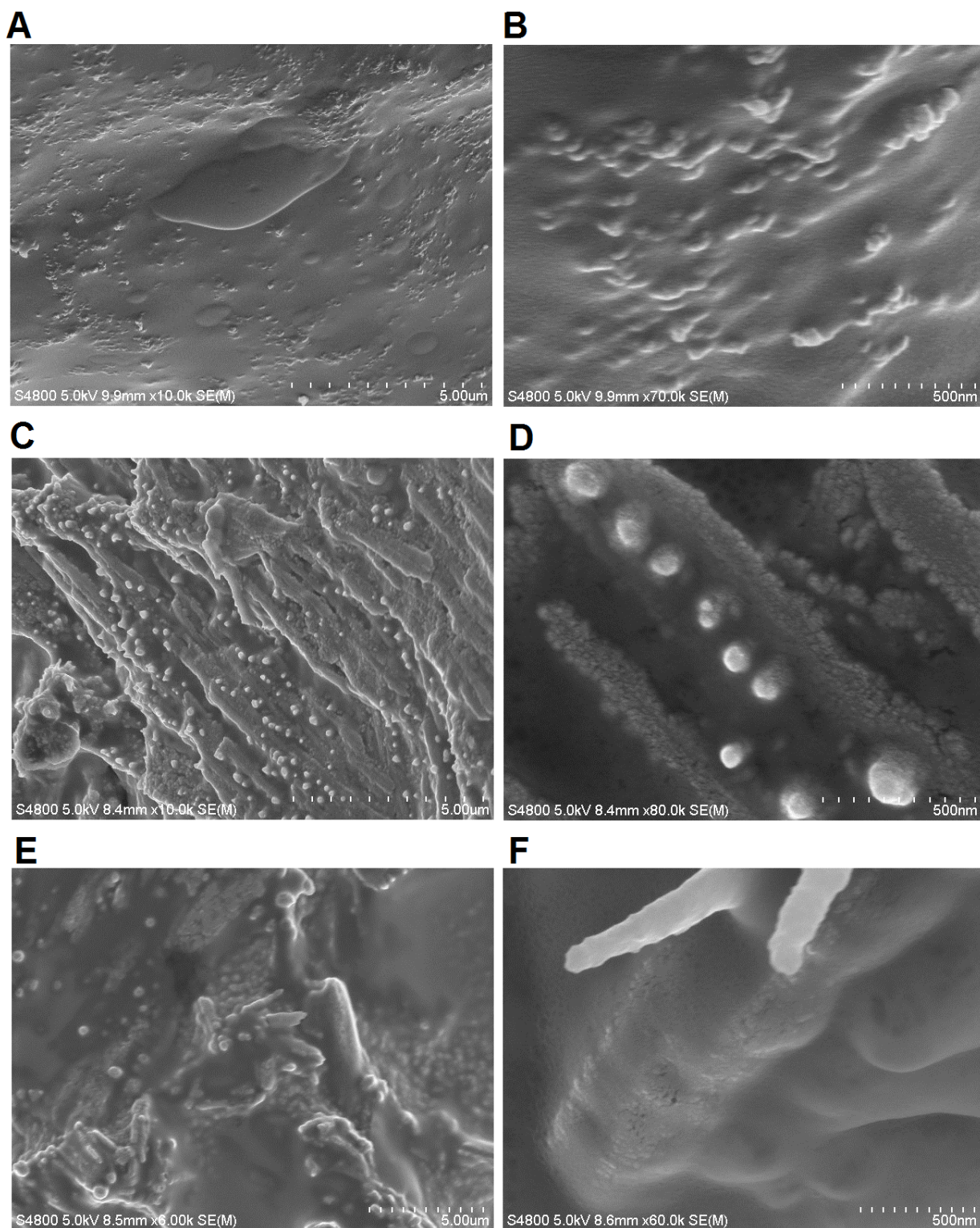


Fig. 9 SEM images of **Bp-Ty 2** polymer (A, B) and the polyplex with 0.5:1 polymer-DNA ratio (C, D) and 1:1 polymer-DNA ratio (E, F).

Cite this: DOI:

10.1039/c0xx00000x

www.rsc.org/xxxxxx

ARTICLE TYPE

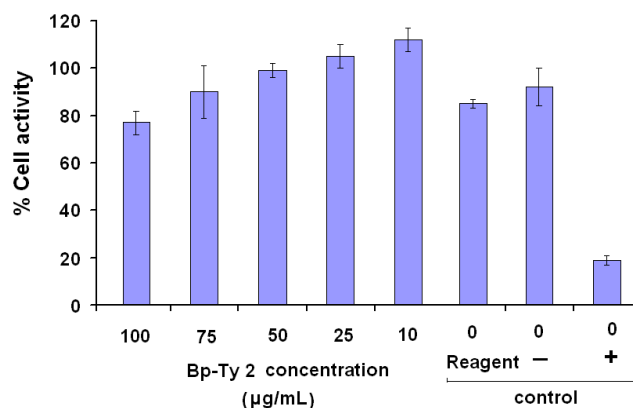


Fig. 10 Percentage cellular metabolic activity of the polymer **Bp-Ty 2** with L929 mouse fibroblast cells at different concentrations of **Bp-Ty 2** after 24 hours of incubation. Positive control contains UHMWPE and negative control contains dilute phenol.

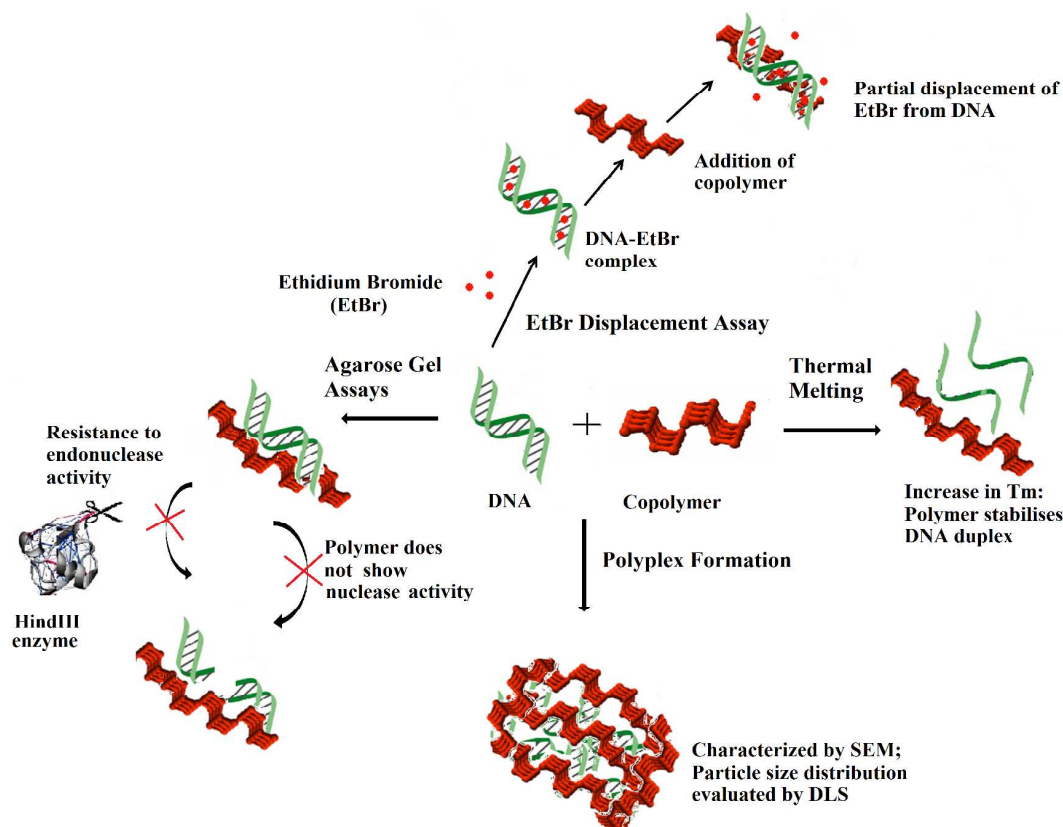
Cell viability

Tyrosine-based polymers have been previously reported to be non-cytotoxic.⁹ In the present study, the cell viability of L929 mammalian cells (mouse fibroblast) incubated with the

10 copolymer **Bp-Ty 2** was evaluated by assessment of the cell metabolic activity (MTT assay). The metabolic activity of the cells in the presence of **Bp-Ty 2** in the concentration range 10-100 µg/mL is seen to remain high (Figure 10).

At 100 µg/mL concentration of **Bp-Ty 2**, the metabolic activity is 15 close to the reagent control and significantly higher than the negative control phenol, which is indicative of low cytotoxicity of the polymer at this concentration. At lower concentrations of 10-75 µg/mL, the metabolic activity is observed to be greater, even higher than the reagent control that does not contain any polymer.

20 This signifies that in the presence of the polymer at relevant concentrations, the normal functioning of the cells are not interrupted. Overall, the synthesized polymer is observed to be non-cytotoxic at reasonable concentrations. The biocompatibility of the polymer is noticeable even in the presence of DGEBA 25 moieties, probably owing to the occurrence of the tyrosine units. In case the polymer find applications in vector delivery in future, its non-cytotoxicity may be an advantageous property since commonly used few PEIs have been reportedly found to be cytotoxic^{26,30}.



30

Scheme 2 Scheme visualising the interaction of the copolymer with DNA via EtBr displacement assay and thermal melting at the interface and DNA-polymer complex formation as indicated by DLS and SEM

Cite this: DOI:

10.1039/c0xx00000x

www.rsc.org/xxxxxx

ARTICLE TYPE

Conclusions

DGEBA and Tyrosine derived **Bp-Ty** copolymers with different monomer ratios were synthesized successfully using DMAP as a catalyst. Characterization of the polymer was done by FTIR spectroscopy that indicates presence of characteristic wavelengths for both the starting materials as well as the formation of carbonyl bonds. ¹H and ¹³C NMR indicated presence of carbonyl linkages and the former also displayed aliphatic to aromatic proton ratio close to 1:2. Thermal degradation studies confirmed the monomer ratios as 0.49:1, 1:1 and 1.1:1 in the synthesised polymers **Bp-Ty 1, 2** and **3** with an equimolar content of Tyrosine with DGEBA as the maximum incorporated in the polymers. Cell viability studies performed using the MTT assay confirmed the non-cytotoxic nature of the polymer.

The **Bp-Ty 2** polymer was thus studied with DNA to ascertain its employability in biological applications. Our experiments indicate possible formation of polyplex at relevant concentration of the DNA and the polymer. The polymer was found to increase the melting temperature by 4°C, thereby lending stability to the DNA after polyplex formation. Agarose gel assays proved that the polymer does not damage the DNA and even offer resistance to endonuclease activity, a fact promising for its potential bioapplications. Fluorescence assay conducted with the intercalated EtBr suggested partial intercalation or groove binding of the polymer with the DNA helix at higher polymer concentrations. DLS experiments showed stable particle formation at polymer-DNA ratios of 1:1 till 5:1 and a decrease in zeta potential of the polymer upon complexation with DNA. The polymer-DNA conjugate was imaged on SEM that displayed clusters of DNA spread discreetly on the polymer sheet. Overall, a novel and biocompatible polymer with DGEBA and tyrosine was created and characterized. The interaction of the polymer with DNA was evaluated that gave important insights regarding its potential to be used in biological applications. In particular, our studies indicate that the polymer has potential biological applications including but not limited to scaffolding and vector delivery.

Acknowledgements

RM is thankful to Bridgestone Corporation (Japan) for fellowship and RK is thankful for fellowship to IIT Patna. The authors are thankful to SAIF Panjab University for NMR Spectroscopy and IISc Bangalore for ESI-Mass Spectrometry. The authors are also thankful to SCTIMST, Trivandrum for conducting MTT Assay to determine cell viability. Financial assistance from Dept. of Science and Technology, Govt. of India (grant no. SR/FT/LS/36/2010) to PD is gratefully acknowledged.

Notes and references

^a Department of Chemistry, Indian Institute of Technology, Patna, India-800013.

^b Department of Material Science, Indian Institute of Technology,

Patna, India- 800013.

*Corresponding Author E-mail Address: director@iitp.ac.in, anilkb@rtc.iitkgp.ernet.in; Fax: +91-6122277384; Tel: +91-6122277380.

Electronic Supplementary Information (ESI) available: Mass Spectrometry figure, TGA derivative curves, Differential Scanning Calorimetry Data, Agarose assay with PEI, DLS data for 30 minutes and pKa and ionization of the polymer. See DOI: 10.1039/b000000x/

- [1] M. Levitt, S. Spector, A. Sjoerdsma, and S. Udenfriend, *J Pharmacol Exp Ther*, 1965, **148**, 1
- [2] S. Meyers, *Altern Med Rev*, 2000, **5**, 64.
- [3] S. Udenfriend and J. B. Wyngaarden, *Biochim Biophys Acta*, 1956, **20**, 48.
- [4] J. D. Elsworth and R. H. Roth, *Exp Neurol*, 1997, **144**, 4.
- [5] B. A. Barry and G. T. Babcock, *Proc Natl Acad Sci U S A*, 1987, **84**, 7099.
- [6] (a) V. Tangpasuthadol, A. Shefer, K. A. Hooper, and J. Kohn, *Biomaterials*, 1996, **17**, 463; (b) M. H. R. Magno, J. Kim, A. Srinivasan, S. McBride, D. Bolikal, A. Darr, J. Hollinger and J. Kohn, *J Mat Chem*, 2010, **20**, 888; (c) J. Rickerby, R. Prabhakar, M. Ali, J. Knowles, and S. Brocchini, *J Mat Chem*, 2005, **15**, 1849.
- [7] A. S. Gupta and S. T. Lopina, *J Biomater Sci Polym Ed*, 2002, **13**, 1093.
- [8] G. Creusat, A. S. Rinaldi, E. Weiss, R. Elbaghdadi, J. S. Remy, R. Mulherka and G. Zuber, *Bioconjug Chem*, 2010, **21**, 994.
- [9] S. L. Bourke and J. Kohn, *Adv Drug Deliv Rev*, 2003, **55**, 447.
- [10] A. Sen Gupta and S. T. Lopina, *Polymer*, 2005, **46**, 2133.
- [11] D. Y. Sarkar, J.-C., N. Klettlinger, and S. T. Lopina, *EXPRESS Polymer Letters*, 2007, **1**, 724.
- [12] F. E. Ali, K. J. Barnham, C. J. Barrow, and F. Separovic, *J Inorg Biochem*, 2004, **98**, 173.
- [13] C. Troiber, D. Edinger, P. Kos, L. Schreiner, R. Kläger, A. Herrmann and E. Wagner, *Biomaterials*, 2013, **34**, 1624.
- [14] L. González, X. Ramis, J. M. Salla, A. Mantecón, and A. Serra, *J Appl Pol Sci*, 2009, **111**, 1805.
- [15] M. Arasa, X. Ramis, J. M. Salla, A. Mantecón, and A. Serra, *Polymer*, 2009, **50**, 2228.
- [16] I. E. Dell'Erba and R. J. J. Williams, *Polymer Eng & Sci*, 2006, **46**, 351.
- [17] N. Roy and A. K. Bhowmick, *Polymer*, 2010, **51**, 5172.
- [18] H. Datta, A. K. Bhowmick, and N. K. Singha, *Polymer*, 2009, **50**, 3259.
- [19] (a) T. Fukuoka, Y. Tachibana, H. Tonami, H. Uyama, and S. Kobayashi, *Biomacromolecules*, 2002, **3**, 768; (b) L. H. Jones, A. Narayanan, and E. C. Hett, *Molecular BioSystems*, 2014, **10**, 952.
- [20] U. Rungsardthong, T. Ehtezazi, L. Bailey, S. P. Armes, M. C. Garnett, and S. Stolnik, *Biomacromolecules*, 2003, **4**, 683.
- [21] C. Yu and J. Kohn, *Biomaterials*, 1999, **20**, 253.
- [22] A. Choudhury, A. K. Bhowmick, and C. Ong, *J Appl Pol Sci*, 2010, **116**, 1428.
- [23] S. J. Tseng and S. C. Tang, *Biomacromolecules*, 2007, **8**, 50.
- [24] A. Schallon, C. V. Synatschke, D. V. Pergushov, V. Jérôme, A. H. Müller, and R. Freitag, *Langmuir*, 2011, **27**, 12042.
- [25] V. H. Mulimani and R. A. Day, *Indian J Biochem Biophys*, 1982, **19**, 292.
- [26] X. Yan, Y. Zhang, H. Zhang, P.G. Wang, X. Chu and X. Wang, *Org Biomol Chem*, 2014, **12**, 1975.

-
- [27] S. J. Hwang, N. C. Belloq, and M. E. Davis, *Bioconjug Chem*, 2001, **12**, 280. [30] (a) M. Thomas and A.M. Klibanov, *Proc Natl Acad Sci U S A*, 2002, **99**, 14640; (b) S.M. Moghimi, P. Symonds, J.C. Murray, A.C. Hunter, G. Debska and A. Szewczyk, *Mol Ther*, 2005, **11**, 990.
- [28] V. A. Bloomfield, *Biopolymers*, 1997, **44**, 269.
- [29] F. K., Y. K. Luu, M. Hadjiargyrou, and D. Liang, *PLoS ONE*, 2010, **5**, 13308. 10